



Research Article

IN SILICO ASSESSMENT OF FLAVONOIDS FROM MATRICARIA CHAMOMILLA FOR ANTI-PSORIATIC POTENTIAL VIA MOLECULAR DOCKING AND ADME/T PROFILING

V. V. Rajesham¹, Narendra Pentu^{2*}, Pasupuleti Kishore Kumar¹, T. Rama Rao², Ashok Morsu³

Article Information

Received: 10th May 2025
Revised: 27th July 2025
Accepted: 11th August 2025
Published: 31st August 2025

Keywords

Molecular docking, Psoriasis, Flavonoids, Phytochemicals, Matricaria Chamomilla, Redocking, ADME/T profiling.

ABSTRACT

Background: Computational tools are advancing in the drug discovery process to assess the safety profiles of new compounds with reduced investment. Herbal remedies exhibit a diverse range of active compounds that can alleviate various disease conditions with fewer side effects. **Method:** This study investigates the molecular docking of phytochemicals from *Matricaria Chamomilla* against inflammation-induced skin disorders, such as psoriasis. Using AutoDock Vina and MGL Tools, key compounds were evaluated for binding affinity with target proteins. ADMET analysis, as assessed by pkCSM and SWISSADME, to predict the Lipinski's Rule of Five. Redocking was implemented to confirm the binding affinity of the docked position. **Results:** This molecular docking of phenolic compounds and flavonoids, including quercetin, apigenin, rutin, luteolin, and various glycosylated derivatives—from *Matricaria Chamomilla* against cellular proteins implicated in psoriasis (PDE-4, p38MAPK, IL-23, BTK, JAK-3, TNF- α , IL-17A, and IL-6). Using Autodock Vina and MGL Tools, rutin and quercetin demonstrated favourable binding affinities. At the same time, luteolin-7-glycoside exhibited the highest docking scores (e.g., -10.8 kcal/mol for PDE-4, -9.7 kcal/mol for JAK-3, and -9.1 kcal/mol for TNF- α) compared to the standard. Results highlight the potential of chamomile phytochemicals as safe, orally effective agents for managing inflammatory skin conditions. Redocking confirms the RMSD values are within the limits of $< 2 \text{ \AA}$. **Conclusion:** The data suggest that chamomile flavonoids could be safe and beneficial for treating inflammatory diseases and psoriasis. Although enzymatic and cell-based assays, along with further preclinical evaluations, are essential for advancing research in disease modification, formulation strategies play a role in improving drug characteristics.

INTRODUCTION

Psoriasis is a chronic, inflammatory skin disorder that can occur at any age, regardless of gender. Inflammation is the major

disease propagation condition in psoriasis, a skin inflammation disorder [1]. The disease condition is characterized by the

¹Department of Pharmacology, CMR College of Pharmacy, Kandlakoya (V), Medchal, Hyderabad, Telangana-501401.

²Department of Pharmaceutics, CMR College of Pharmacy, Kandlakoya (V), Medchal, Hyderabad, Telangana-501401.

³PPD part of Thermo Fischer Scientific, 3900 Paramount Parkway, Morrisville N.C. 27560.

*For Correspondence: narendrapentu@gmail.com

©2025 The authors

This is an Open Access article distributed under the terms of the Creative Commons Attribution (CC BY NC), which permits unrestricted use, distribution, and reproduction in any medium, as long as the original authors and source are cited. No permission is required from the authors or the publishers. (<https://creativecommons.org/licenses/by-nc/4.0/>)

scaling of skin layers, itching, dryness of the skin, and hair loss, primarily affecting the trunk and joint regions. Psoriasis is a chronic disorder that can be influenced by lifestyle factors and may also be triggered by genetic conditions. Immunological studies suggest that secondary signaling mechanisms mediated by pro-inflammatory cytokines, such as IL-17 and IL-6, play a central role in the pathogenesis and disease progression of psoriasis. These cytokines initiate downstream chemical signalling cascades that activate keratinocytes, dendritic cells, and T-helper cells, thereby perpetuating a chronic inflammatory cycle. The activation of the JAK/STAT, MAPK, and NF- κ B pathways further amplifies the inflammatory response, leading to epidermal hyperproliferation and dysfunction of the skin barrier. Thus, IL-17 and IL-6 are considered critical therapeutic targets for modifying the disease in the management of psoriasis. [2]. Psoriasis affects approximately 125 million people worldwide, with the highest prevalence rate among adults aged 35-55 years. According to a study, countries closer to the equatorial regions are less prone to psoriasis disease, indicating that environmental factors also play a significant role in disease occurrence [3]. Although the definitive gene causing psoriasis has not been identified, research findings are revealing that the occurrence of significant genetic diseases is associated with the PSOR-1 to 9 genes. Anxiety and depression affect 1/4th of psoriasis patients; unfortunately, it is missing in clinical findings. Cardiovascular and skin cancer diseases are the major comorbidities associated with psoriasis for long-term phototherapy treatment [4]

Chamomile is derived from the native source *Matricaria Chamomilla*, a member of the Asteraceae family. *M. Chamomile* flowers produce 0.2 to 1.9% Blue essential oils and flavonoids. It is widely used as an anti-inflammatory agent, and it is believed to be the root cause of several internal disorders, modifying the disease condition. Names like German chamomile, Hungarian chamomile, Babunji, and Roman chamomile well know chamomile [5]. German chamomile acts as a therapeutic agent in treating various inflammations and cramps. Apart from this, it is active in treating anxiety and cancer. Wound healing properties and skin barrier nature increased the scope of the compounds in treating several skin-related inflammations [6]. The major phytoconstituents of *Matricaria Chamomilla* include sesquiterpenes such as α -bisabolol, matricin, chamazulene, and farnesene derivatives (farnesene, β -farnesene, farnesol), along with phenolic acids (caffeic acid, chlorogenic acid), coumarins

(umbelliferone, herniarin), and flavonoids (apigenin, luteolin, quercetin, and apigenin-7-O-glucoside). In addition, esters such as isobutyl angelate and 2-methyl butyl angelate contribute to its pharmacological properties. Flavonoids of various subclasses exhibit anti-inflammatory, anti-oxidative, and inhibitory effects on keratinocyte hyperproliferation. Some of the selected flavonoids have the potential to inhibit the cytokine production and infiltration of immune cells. Psoriasis disease progression is continued by the evidence of crosstalk between innate and adaptive immune reactions triggered by the TNF-Alpha, interleukin, and interferon Gamma [7]. Continuous production of T cells, which migrate into the epidermis, further releasing cytokines that affect T helper cells 1 and 17. IL-17 and IL-23 are the major proteins that trigger cytokine production and activate the keratinocyte proliferation mechanism.

Polyphenol class flavonoids have the potential to interfere with the signalling mechanism at the molecular level related to many abnormal functions. The skin is the outermost organ of our body, and it maintains communication with internal immune cells, such as skin-associated lymphoid tissue cells (SALT), which include keratinocytes, T lymphocytes, vascular endothelial cells, macrophages, and mast cells. Chemokines and cytokines initiate the inflammation reactions to maintain the integrity and homeostasis of the skin. The uppermost layer of skin, the epidermis, is non-vascularized, highly keratinized, and is responsible for maintaining the elasticity of skin layers. Flavonoids act on the keratinized skin layers to restore the skin layer's integrity and reduce the proliferation of skin cells [8]. This study investigates the flavonoids present in Chamomile (*Matricaria Chamomilla* L.) and their therapeutic effects on inflammatory skin diseases, particularly psoriasis, supported by molecular docking studies and pharmacokinetic analyses.

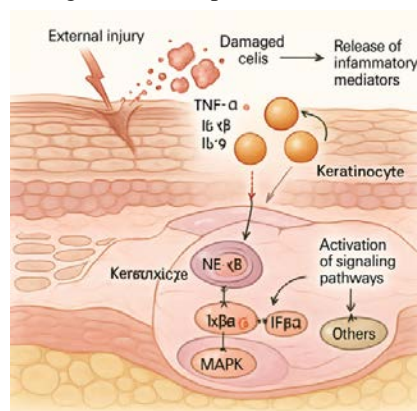


Figure 1: Diagrammatic representation of Cytokines' involvement in Keratinocyte proliferation

MATERIALS AND METHODS

The article by Ompal Singh et al. (2010, "Chamomile: an overview") provides a comprehensive and detailed description of the plant's chemical constituents, facilitating study and research into its various activities. This work aims to provide a comprehensive picture of the anti-psoriatic activity of the chemical constituents present in chamomile. German chamomile has been used to treat skin-related inflammatory diseases [9]. So far, several alternative allopathic treatments are available for immediate relief, but not permanent. Although herbal treatment is very cost-effective, it has fewer long-term side effects, thereby maintaining the patient's quality of life. Ligands are selected from the Ompal Singh review article, out of the total chemical constituents' majority portion occupied by the flavonoids and terpenoids. A list of ligands is given in the table, and the energy levels are reduced to the minimum for stable bond formation. Molecular docking was performed on a system running 64-bit Windows 11, equipped with 16 GB of RAM and a 13th Generation Intel Core i5-1335U processor (1.30 GHz, x64 architecture).

Molecular docking

Virtual screening of the molecules was performed using software tools like AutodockVina, with protein molecules downloaded from the Protein Data Bank (<https://www.rcsb.org/>). All the crystallized structures were selected in Homosepians' selectivity. Discovery studio was used to visualize the protein molecule; all ligand molecules were identified, and pre-associated ligands were removed by calculating the GRID coordinates. Ligand molecules downloaded from the PubChem site in SDF format are converted to the PDB. file format. Docking was done for the ligand and protein molecule with AutodockVina software [10]. The resulting coded structures were analyzed by using the Maestro suite of Schrodinger software and Discovery Visualizer [11] [12]. The docking mechanism can be explained in three steps: 1) selection of proteins and their preparation. 2) Predict the active site of binding in the receptor protein with the ligand and receptor-based drug design. 3) Analyze the binding affinity and bond length. Selection of proteins is based on the pathophysiology and selective signalling pathways involved in disease progression. Here, ligands were flavonoids, based on the structural components' activity against the various pharmacological actions, and it was selected. The selected proteins were visualized in Discovery Studios, and the water

molecules and small molecules were removed. The active site of prediction is accessed by generating a GRID box using a blind docking mechanism, based on the native ligand location of binding to the protein. Based on the docking score, the bond strength was analyzed [13]. Here, methotrexate is used as the standard drug to compare the binding affinity of the flavonoids.

Redocking and its validation mechanism

The redocking mechanism is an essential validation step in molecular docking studies. It evaluates whether a docking algorithm can successfully replicate the experimentally determined binding pose of a ligand within a protein's active site. The process involves several sequential steps: preparing the structures, removing the ligand from the binding site, performing the redocking, predicting and scoring the binding poses, validating the docked pose against the experimental structure, and interpreting the results by calculating the root mean square deviation (RMSD) between the predicted and experimental ligand positions. An RMSD value of 2.0 Å or less is commonly accepted as indicative of successful redocking.

Drug likeliness assessment

The rule of five (Ro5) is used to assess the oral bioavailability of compounds. Lipinski's rule of five encompasses properties such as molecular weight, Hydrogen bond donor, hydrogen bond acceptor, and lipophilicity, all within specific limits, to demonstrate good bioavailability characteristics [14].

Pharmacokinetic parameters and toxicity studies

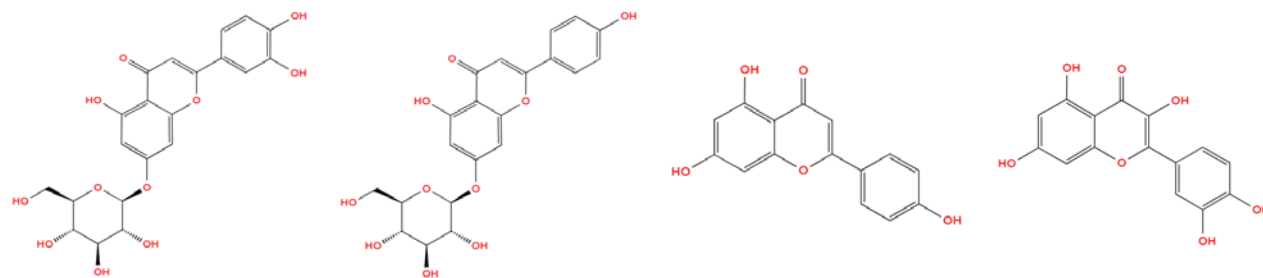
All the possible physicochemical descriptors are calculated by using SWISSADME, DruLito, and pkCSM software. Various ADME/T properties were evaluated to determine the safety profiles of the compounds. The drug discovery process is the initial step in identifying the potential effectiveness of compounds against the causative agents. Furthermore, these data are used in clinical trials to inform the design of the dosage form. ChemDraw Professional 16.0 software is used to draw the structures [15][16].

RESULTS AND DISCUSSION

Docking studies conducted using software tools are crucial in the drug discovery process for analyzing the structural orientation and arrangements of ligands within protein sockets. The information obtained from the tools serves as a reliable source for comparison with the experimental data points. Consistent

amino acid binding was observed in several compounds, suggesting the capacity of the docking site and aiding in study optimization [17]. Flavonoids are the primary source of the plant

Matricaria chamomile & these compounds' 2D structures are represented in Figure 2.



Luteolin-7-o-glucoside

Apigenin-7-o-glucoside

Apigenin

Quercetin

Figure 2: 2D-chemical structures of flavonoids from *Matricaria Chamomilla*.

Docking Score calculation and bonding strength evaluation

Ligands identified from the source plant of *Matricaria Chamomilla* are 16 in number, docked with the 8 protein molecules of psoriatic disease, docking scores of the ligands, and the highest docked ligands to the number of proteins are represented in the table and figure. Number of ligands includes flavonoids like quercetin, apigenin, apigenin-7-glucoside, luteolin, luteolin-7-glucoside [18], matricin (sesquiterpene lactone), Chamazulene (terpenoid) [19], Caffeic acid (Polyphenol)[20], Guaiazulene (azulenes) [21] Isobutyl angelate (fatty acid ester), Farnesene, Beta-farnesene, Farnesol, alpha-Bisabolol (acyclic sesquiterpene) [22] Umbelliferone (coumarin) [23], Herniarin (substituted coumarins at 7-methoxy positions) [24].

All the flavonoid-related compounds like quercetin, apigenin, luteolin, flavonoid, and glycosides like apigenin-7-glycoside, luteolin-7-glycoside show the highest docking score when compared with other ligands like coumarins, azulenes, sesquiterpenes, and polyphenols. In flavonoid molecules, the highest docked proteins are luteolin-7-glucoside with a docking score of -10.8 (PDE-4), -10.1(BTK), -9.7 (JAK-3), -9.1 (TNF- α). Apigenin-7-glucoside with docking score of -10.7 (PDE-4), -9.9 (BTK), -9.5 (JAK-3), -8.8 (TNF- α).

Due to the glycosidic linkage of flavonoid compounds, the bonds are stronger than the flavonoid compounds. 13 out of 15 ligands are bonded with the highest docking score with PDE-4 protein, 11 bonded with JAK-3, 9 docked with BTK, 6 docked with TNF- α , and IL-17A protein. Farnesene, isobutyl angelate, shows a

lower docking score & an average docking score of -6.5 K.Cal/ Mol. TNF- α is Tumor necrosis factor Alpha (PDB: 2AZ5), IL-23 is Interleukin-23 (PDB: 3QWR), IL-17A is interleukin 17 A (PDB: 5HI4), PDE-4 is Phosphodiesterase-4 (PDB: 5K11), BTK is Bruton's tyrosine kinase (PDB ID: 4OTF), JAK-3 is Janus kinase (PDB: 5TTS), IL-6 is interleukin- 6 (PDB ID: 5FUC), P38MAPK is mitogen activated protein kinase p38 (PDB: 2C6O). No interactions are observed between IL-23 and p38 MAPK. IL-6 has significantly few interactions, like 5 out of 15 ligands. In flavonoids, a sugar molecule with a higher polar nature forms a strong bonding behavior with the targeted proteins [25].

An increased number of hydroxyl groups increases the binding affinity towards the proteins. Lipophilic group attachment significantly enhances the docking score compared to polar head groups. More violations are observed in the Lipinski rule, as per the rule of five, in luteolin-7-glucoside due to violations in Hydrogen bond acceptors and donors.

An increase in the number of hydrogen bond acceptors (HBA) and hydrogen bond donors (HBD) may reduce a molecule's lipophilicity, making it more difficult to permeate through the skin layers. This limited permeability can lead to increased deposition of the compound in the upper layers of the skin. This strategic approach is helpful in managing skin-related inflammatory disorders such as psoriasis, as increased deposition of therapeutic compounds in the upper skin layers can enhance local efficacy where inflammation occurs [26]. Hydrogen bond donors and acceptors in chemical structures

serve as critical points of interaction that govern solubility, stability, delivery, retention, and biological activity of molecules [27][28]. P38MAPK, JAK-3, and IL-23 did not generate any covalent hydrogen bonds during receptor-ligand interactions. IL-6 formed some hydrogen bonds (THR A:218) with all of the ligands, including the methotrexate molecule. BTK protein with MET A:47 hydrogen bonds. IL-17A and PDE-4 formed

hydrogen bonds with various amino acids. Amino acid interactions in proteins are classified into hydrogen and non-hydrogen bonds, which are identified by colored lines. Light green colour- van der Waals, green-Hydrogen bond, light pink-Pi-alkyl, pink- Pi-Pi bond, orange-Pi-sulfur bonds. In Table 3, the bonding of flavonoidal compounds to receptors is indicated by both hydrogen and non-hydrogen bonds.

Table 1: Molecular docking binding affinities (kcal/mol) of ligands with the protein targets involved in Psoriasis.

S. No.	TNF- α	IL-23	IL-17A	PDE-4	BTK	JAK-3	IL-6	P38MAPK
Quercetin	-7.4	-5.8	-7.1	-8.8	-8.2	-8.4	-7.2	-5.6
apigenin	-7.3	-5.7	-7.2	-8.6	-8.6	-8.3	-6.8	-5.7
Apigenin 7-glucoside	-8.8	-6.1	-8.0	-10.7	-9.9	-9.5	-6.9	-5.9
Luteolin	-7.4	-5.9	-7.4	-8.5	-8.8	-8.6	-7.2	-5.6
Luteolin-7-O-glucoside	-9.1	-6.2	-8.2	-10.8	-10.1	-9.7	-7.0	-5.1
Matricin	-6.5	-5.9	-7.7	-8.5	-8.1	-8.2	-6.1	-5.8
Chamazulene	-5.7	-5.4	-6.4	-8.5	-7.5	-8.2	-5.3	-5.1
Caffeic acid	-5.4	-4.5	-5.4	-6.6-7.0	-6.4	-6.6	-5.5	-5.0
Guaiazulene	-6.2	-5.6	-6.8	-8.7	-7.7	-8.5	-5.6	-5.2
Isobutyl angelate	-4.4	-4.2	-4.3	-5.5	-4.7	-5.3	-4.2	-4.4
Farnesene	-5.3	-4.2	-5.4	-6.3	-6.3	-6.0	-5.1	-4.3
Beta-farnesene	-5.2	-3.8	-5.4	-6.6	-5.3	-6.0	-5.0	-4.8
Farnesol	-5.7	-4.4	-5.3	-6.8	-6.0	-6.3	-4.9	-4.4
alpha-Bisabolol	-5.7	-5.2	-6.4	-7.0	-6.3	-6.4	-5.2	-5.0
Umbelliferone	-5.5	-4.8	-5.8	-6.9	-6.5	-6.7	-5.6	-4.8
Herniarin	-5.6	-4.7	-5.9	-7.0	-6.4	-6.7	-5.5	-4.9
Methotrexate	-8.1	-7.7	-6.7	-8.2	-6.4	-8.3	-7.9	-7.1

TNF- α : Tumor necrosis factor Alpha; IL-23: Interleukin 23; IL-17A: Interleukin 17A; PDE-4: Phosphodiesterase 4; BTK: Bruton's Tyrosine Kinase; JAK-3: Janus Kinase 3; IL-6: Interleukin 6; p38MAPK: p38 mitogen-activated protein kinase.

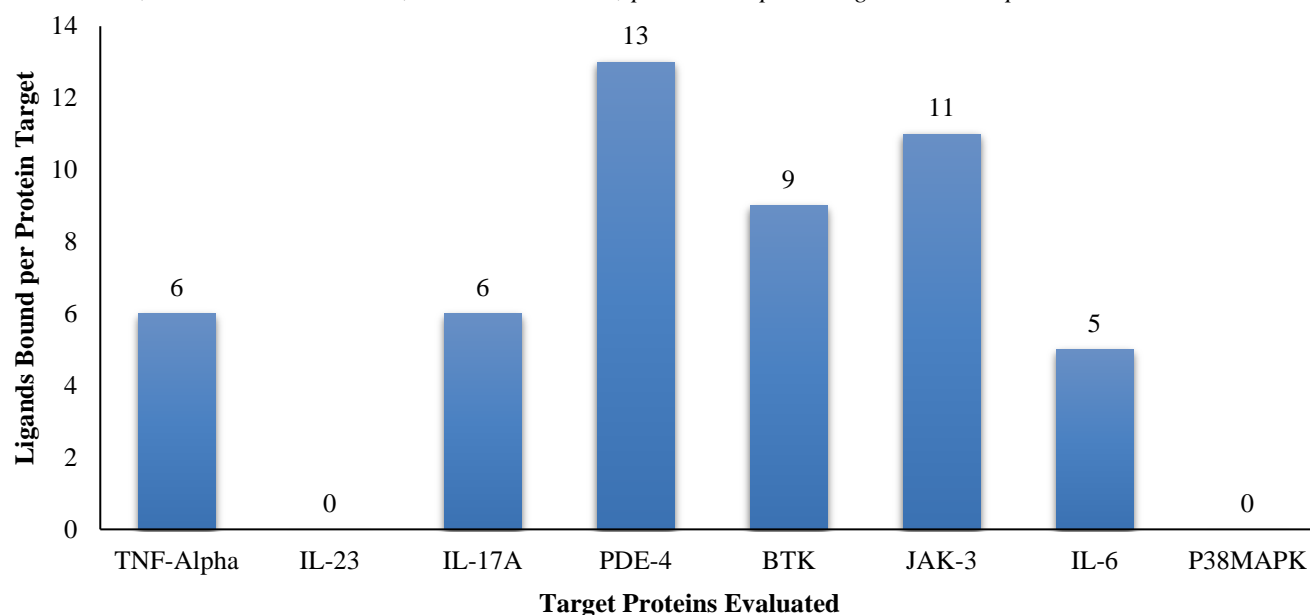
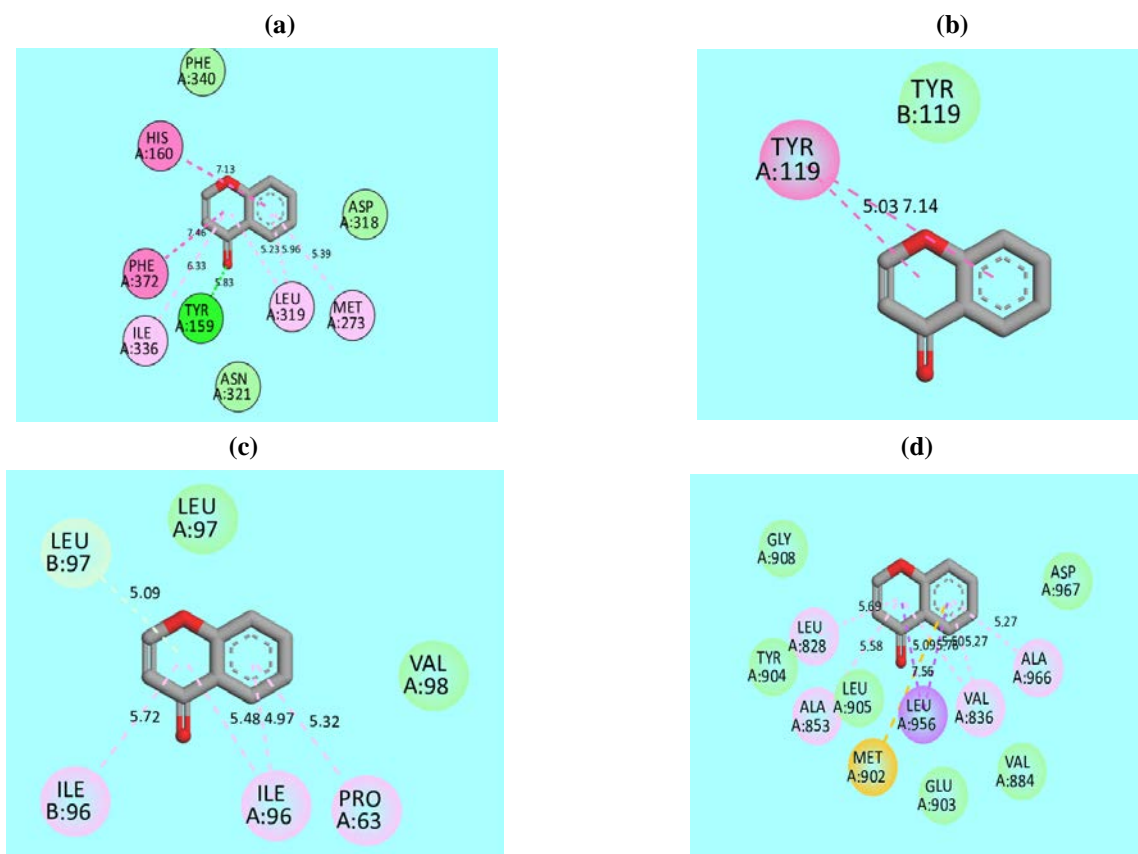


Figure 3: Number of ligand binding to key inflammatory protein targets involved in psoriasis.

Table 2: Physicochemical properties of key bioactive ligand from chamomile

S. No.	Compound	HBA	HBD	Mol. Wt	X logP	R.Bonds	TPSA	LV																																				
1	Quercetin	7	5	302.238	1.988	1	122.108	0																																				
2	apigenin	5	3	270.24	2.5768	1	112.519	0																																				
3	Apigenin 7-glucoside	10	6	432.218	0.0499	4	174.313	2																																				
4	Luteolin	6	4	286.239	2.2824	1	117.313	0																																				
5	Luteolin-7-O-glucoside	11	7	448.38	-0.2445	4	179.107	2																																				
6	Matricin	5	1	306.358	1.753	1	129.526	0																																				
7	Chamazulene	0	0	184.282	3.97	1	85.927	0																																				
8	Caffeic acid	3	3	180.271	1.195	2	74.38	0																																				
9	Guiazulene	0	0	198.309	4.53	1	92.29	0																																				
10	Isobutyl angelate	2	0	156.225	2.15	3	68.244	0																																				
11	Farnesen	0	0	204.357	5.20	6	95.09	0																																				
12	Beta-farnesene	0	0	204.357	5.20	7	95.09	0 </tr <tr> <td>13</td> <td>Farnesol</td> <td>1</td> <td>1</td> <td>222.37</td> <td>4.39</td> <td>7</td> <td>100.57</td> <td>0</td> </tr> <tr> <td>14</td> <td>alpha-Bisabolol</td> <td>1</td> <td>1</td> <td>222.37</td> <td>4.23</td> <td>4</td> <td>100.258</td> <td>0</td> </tr> <tr> <td>15</td> <td>Umbelliferone</td> <td>3</td> <td>1</td> <td>162.144</td> <td>1.49</td> <td>0</td> <td>67.87</td> <td>0</td> </tr> <tr> <td>16</td> <td>Herniarin</td> <td>3</td> <td>0</td> <td>176.171</td> <td>1.80</td> <td>1</td> <td>74.55</td> <td>0</td> </tr>	13	Farnesol	1	1	222.37	4.39	7	100.57	0	14	alpha-Bisabolol	1	1	222.37	4.23	4	100.258	0	15	Umbelliferone	3	1	162.144	1.49	0	67.87	0	16	Herniarin	3	0	176.171	1.80	1	74.55	0
13	Farnesol	1	1	222.37	4.39	7	100.57	0																																				
14	alpha-Bisabolol	1	1	222.37	4.23	4	100.258	0																																				
15	Umbelliferone	3	1	162.144	1.49	0	67.87	0																																				
16	Herniarin	3	0	176.171	1.80	1	74.55	0																																				

HBA: Hydrogen bond acceptors; HBD: Hydrogen bond donors; XLogP: Partition coefficient value; R.bonds: Rotatable bonds; TPSA: Total polar surface area; LV: Lipinski's rule violations.



Pink: Indicates π - π stacking interactions between the ligand and amino acid side chains., **Purple:** Represents π -sigma interactions (π - σ bonds) with the ligand., **Light Pink:** Denotes π -alkyl interactions involving the ligand and amino acid alkyl groups., **Orange:** Corresponds to π - π -sulfur interactions between the ligand and sulfur-containing residues.

Figure 4: Ligand-protein binding interactions: amino acid residue mapping luteolin-7-glucoside with (a) PDE-4, (b) TNF-Alpha, (c) IL-17A, and (c) JAK-3 proteins.

Table 3: Representation of receptor and ligand interactions with hydrogen and non-hydrogen bonding.

Protein	Ligands	Hydrogen Bonds	Non-hydrogen bonds
TNF-α (2AZ5)	Quercetin (5280343)	TYR A:151	TYR A:119; GLN A:61
	Apigenin (5280443)	TYR A:151	TYR A:59; GLN A:61, TYR A:119, LEU A:120, GLY A:121
	Apigenin-7-glucoside (5280704)	-	TYR A:59, GLY A:121, LEU A:120, LEU A:57, LEU B:57.
	Luteolin (5280445)	-	TYR A:119, TYR B:119, TYR A:151, GLN A:61
	Luteolin-7-O-glucoside (5280637)	-	TYR A:119, TYR B:119,
	Methotrexate (126941)	-	TYR B:119, TYR A:119, GLY B:121
IL-23 (3QWR)	Quercetin	-	TRP A:2, ASN A:200, GLU A:12
	Apigenin	-	-
	Apigenin-7-glucoside	-	-
	Luteolin	-	-
	Luteolin-7-O-glucoside	-	-
	Methotrexate	-	-
IL-17A (5HI4)	Quercetin	-	LEU A:112, LEU A:97, LEU B:97, VAL B:98, PRO B:63, TYR B:62, LEU B:99, LEU B:112, LEU A:99
	Apigenin	PRO B:63	LEU A:97, LEU B:97, VAL B:98, TYR B:62, LEU A:112, ILE B:96
	Apigenin-7-glucoside	LEU A:97	LEU B:97, ILE B:96, ILE A:96, PRO B:63, LEU A:112
	Luteolin	GLN B:94	ILE A:66, PRO A:63, ILE A:96, VAL A:117, VAL A:65, TRP A:67
	Luteolin-7-O-glucoside	LEU B:97	ILE A:97, ILE B:97, PRO A:63, LEU A:97, VAL A:98
	Methotrexate	LEU B:97	ILE B:96, LEU A:97
PDE-4 (5K1I)	Quercetin	TYR A:159, HIS A:164	PHE A:372, ILE A:336, MET A:273, HIS A:160, ASP A:318, LEU A:319, PHE A:340
	Apigenin	GLN A:369	ILE A:336, PHE A:372, PHE A:340, LEU A:319, TYR A:159, ASN A:321, TRP A:332, TYR A:329, THR A:333
	Apigenin-7-glucoside	TYR A:159	PHE A:372, HIS A:160, ILE A:336, LEU A:319, MET A:273, PHE A:340, ASN A:321, ASP A:318
	Luteolin	-	HIS A:204, MET A:273, LEU A:229, HIS A:160, SER A:208, ASN A:209, GLU A:230, ASP A:201
	Luteolin-7-O-glucoside	TYR A:159	PHE A:372, HIS A:160, ILE A:336, LEU A:319, MET A:273, PHE A:340, ASN A:321, ASP A:318
	Methotrexate	-	PHE A:340, HIS A:160, ILE A:336, SER A:208
BTK (4OTF)	Quercetin	THR A: 474	LEU A:528, ALA A:428, LEU A:408, VAL A:416, LYS A:430, VAL A:458, GLU A:475, MET A:477, TYR A:476, GLY A:480
	Apigenin	MET A:477	LEU A:408, VAL A:416, ALA A:428, LEU A:528, GLY A:480, TYR A:476, GLU A:475, THR A:474, LYS A:430
	Apigenin-7-glucoside	MET A:477	LEU A:408, VAL A:416, ALA A:428, LEU A:528, GLY A:480, TYR A:476, GLU A:475, LYS A:430
	Luteolin	MET A:477	LEU A:408, VAL A:416, ALA A:428, LEU A:528, GLY A:480, TYR A:476, GLU A:475, THR A:474, LYS A:430
	Luteolin-7-O-glucoside	MET A:477	LEU A:408, VAL A:416, ALA A:428, LEU A:528, GLY A:480, TYR A:476, GLU A:475, LYS A:430
	Methotrexate	-	OCS A:481, GLY A:411, THR A:410, ASN A:526, ARG A:525.
JAK-3 (5TTS)	Quercetin	-	LEU A:956, LEU A:828, VAL A:836, ALA A:853, CYS A:909, GLY A:908, TYR A:904, LEU A:905
	Apigenin	-	LEU A:828, VAL A:836, LEU A:96, ALA A:853, VAL A:884, ALA A:966, MET A:902, LEU A:905, TYR A:904, GLY A:908.

Protein	Ligands	Hydrogen Bonds	Non-hydrogen bonds
	Apigenin-7-glucoside	-	MET A:902 , LEU A:956, LEU A :828, VAL A: 836, ALA A:853, ALA A:966, GLY A:908, TYR A:904, LEU A:905, GLU A:903, VAL A:884, ASP A:967
	Luteolin	-	LEU A:828, VAL A: 836, ALA A:853, LEU A: 956, GLY A:829, GLY A:908, TYR A:904, LEU A:905.
	Luteolin-7-O-glucoside	-	MET A:902 , LEU A:956, LEU A :828, VAL A: 836, ALA A:853, ALA A:966, GLY A:908, TYR A:904, LEU A:905, GLU A:903, VAL A:884, ASP A:967
	Methotrexate	-	LEU A:956, LEU A :828, VAL A: 836, GLY A:908, LEU A:905, TYR A:904.
IL-6 (5FUC)	Quercetin	THR C:218, THR C:204	ASN E:74, ASN C:202, GLN E:72, GLN C:220
	Apigenin	THR C:218, THR C:204	ASN E:74, ASN C:202, GLN E:72, GLN C:220
	Apigenin-7-glucoside	ASN C: 202	THR C:218, THR C:204, ASN E:74, ASN C:202, GLN E:72, GLN C:220
	Luteolin	THR C:218, THR C:204	ASN E:74, ASN C:202, GLN E:72, GLN C:220
	Luteolin-7-O-glucoside	ANS C:202	THR C:204, GLN E:72, GLN C:220
	Methotrexate	THR C:218	ALA E:75, THR C:204, THR C:206, ASN E:74, ASP E:73
P38MAPK (2C6O)	Quercetin	-	VAL A:18, LEU A:134, ALA A:31, ALA A:144, ILE A:10, LEU A:83, PHE A:82, PHE A:80, VAL A:64, GLU A:81, ASP A:145, LYS A:33.
	Apigenin	-	VAL A:18, LEU A:134, ALA A:144, ALA A:31, VAL A:64, ILE A:10, LEU A:83, PHE A:82, PHE A:80, GLU A:81, ASP A:145, LYS A:33.
	Apigenin-7-glucoside	-	VAL A:18, LEU A:134, ILE A:10, ALA A: 31, PHE A:82, LEU A: 83, GLU A:81, PHE A:80, VAL A:64, ALA A:144, ASP A:145, LYS A:33.
	Luteolin	-	VAL A:18, LEU A:134, ALA A:144, ALA A:31, VAL A:64, ILE A:10, PHE A:82, LEU A: 83, GLU A:81, PHE A:80, ASP A:145, LYS A:33.
	Luteolin-7-O-glucoside	-	LEU A: 134, ILE A:10, ALA A: 31, VAL A: 18, ALA A:144, LEU A: 83, PHE A:82, VAL A:64, GLU A:81, ASP A:145, LYS A:33,
	Methotrexate	-	VAL A:18; GLN A:131; ASP A:86; LEU A:134; ILE A:10

Pink: Indicates π - π stacking interactions between the ligand and amino acid side chains., **Purple:** Represents π -sigma interactions (π - σ bonds) with the ligand., **Light Pink:** Denotes π -alkyl interactions involving the ligand and amino acid alkyl groups., **Orange:** Corresponds to π - π -sulfur interactions between the ligand and sulfur-containing residues.

Pharmacokinetic and toxicity analysis of the flavonoid molecules are represented in Table 4. TPSA should be < 140. Absorption characteristics should be greater than 0.90. intestinal absorption must be >30%, skin permeability > -2.5 considered as low skin permeation. BBB > 0.3 indicates that it easily permeates into the brain region. The ADME/T properties (Refer to Table 5) indicate that CYP is the enzyme-related metabolism. Specifically, CYP1A2 is inhibited by quercetin, apigenin, and luteolin, thereby interrupting the metabolism process. AMES toxicity is the induced mutations in genes [29]. CaCO₂ permeability represents the permeation of human epithelial cells, with a value greater than 0.90, indicating higher permeability.

All flavonoidal compounds have lower water solubility due to the presence of higher nonpolar functional groups. Intestinal absorption of more than 30% represents the higher absorption characteristics. All the flavonoids exhibit P-glycoprotein (Pgp) substrate nature, which enables them to extrude toxins from human body cells, and have a reasonable skin permeation probability based on the logKp score. VDss value between 0.71 and 2.81 represents a good volume of distribution. The reported flavonoidal components have low BBB and CNS permeation. Quercetin, apigenin, and luteolin exhibit CYP1A2 inhibition metabolism. No AMES, hepatotoxicity has been reported with the flavonoidal compounds [30, 31].



Figure 5: Lipinski rule of five drug likeness properties of selected compounds from *Matricaria Chamomilla*. HBA: Hydrogen bond acceptors, HBD: Hydrogen bond donors, logP: Partition coefficient.

Ligand Redocking and Validation

Preparation of Structures

The crystal structure of the target protein, complexed with its native ligand, was obtained from file 3071.pdb, generated using BIOVIA software. The ligand coordinates were extracted directly from this structure and used as the reference for subsequent redocking validation. Redocked ligand poses were obtained from the output file mol Conformer 3D_COMPOUND_CID_5280343.pdbqt_out.pdbqt, generated using AutoDock Vina. The docking protocol produced multiple ligand conformations (models), from which the top-ranked pose (Model 1, Vina result: -7.3) was selected for validation [32].

Redocking Protocol

Before docking, protein preparation involved removing non-standard residues, adding hydrogen atoms, and converting file

formats as necessary. The native ligand was extracted from the original PDB file and prepared for Vina as follows:

Protein and ligand files were converted into the required PDBQT format using OpenBabel and AutoDockTools. The docking grid center and dimensions were assigned to encompass the crystallographic position of the native ligand; the grid parameters were chosen to allow for unbiased sampling of the binding pocket.

Assessment of Redocking Accuracy

To assess the accuracy of the docking protocol, the coordinates of the redocked ligand (Model 1) were compared with the crystallographic ligand positions using root-mean-square deviation (RMSD) calculations:

- Atomic coordinates for both ligand poses were extracted for all heavy atoms.

- Pairwise RMSD values were calculated using the following approach: atomic positions from the crystal structure and the best-docked pose were algorithmically superimposed using the Kabsch algorithm, and the RMSD value was obtained.

Table 4: Pharmacokinetic parameters of the selected compounds from *Matricaria Chamomilla*.

Properties	Quercetin	Apigenin	Apigenin-7-Glucoside	Luteolin	Luteolin-7-Glucoside	
PSA	122.108	112.519	174.313	117.313	1179.107	
AlogP	1.988	2.5768	0.0499	2.2824	-0.2445	
Water Solubility (Log mol/L)	-2.925	-3.329	-2.559	-3.094	-2.716	
CaCo2 Permeability (Log Papp in 10 ⁻⁶ cm/s)	-0.229	1.007	0.33	0.096	0.248	ABSORPTION
Interstinal absorption (human % absorbed)	77.207	93.25	37.609	81.13	37.556	
Skin Permeability (log Kp)	-2.735	-2.735	-2.735	-2.735	-2.735	
P-Glycoprotein substrate	YES	YES	YES	YES	YES	
P-Glycoprotein I Inhibitor	NO	NO	NO	NO	NO	
P-Glycoprotein II Inhibitor	NO	NO	NO	NO	NO	
VDss (log L/Kg)	1.559	0.822	0.342	1.153	0.884	
Fraction unbound (Fu)	0.206	0.147	0.218	0.168	0.224	
BBB Permeability (log BB)	-1.098	-0.734	-1.391	-0.907	-1.564	
CNS Permeability (log PS)	-3.065	-2.061	-3.746	-2.251	-3.93	
CYP2D6 substrate	NO	NO	NO	NO	NO	METABOLISM
CYP3A4 substrate	NO	NO	NO	NO	NO	
CYP1A2 inhibitor	YES	YES	NO	YES	NO	
CYP2C19 inhibitor	NO	YES	NO	NO	NO	
CYP2C9 inhibitor	NO	NO	NO	YES	NO	
CYP2D6 inhibitor	NO	NO	NO	NO	NO	
CYP3A4 inhibitor	NO	NO	NO	NO	NO	
Total clearance (Log ml/min/kg)	0.407	0.566	0.547	0.495	0.478	EXCRETION
Renal OCT2 substrate	NO	NO	NO	NO	NO	
AMES toxicity	NO	NO	NO	NO	NO	TOXICITY
Max. tolerable dose	0.453	0.328	0.515	0.499	0.584	
hERG I inhibitor	NO	NO	NO	NO	NO	
hERG II inhibitor	NO	NO	NO	NO	NO	
Hepatotoxicity	NO	NO	NO	NO	NO	
Skin Sensitization	NO	NO	NO	NO	NO	
Oral rat acute toxicity(LD50) mol/ kg	2.471	2.45	2.595	2.455	2.547	
Oral rat Chronic toxicity (LOAEL)log mg/kg_ bw/day	2.612	2.298	4.359	2.409	4.279	

The RMSD calculated between the crystallographic and redocked ligand poses was approximately 1.10 Å, which is well below the widely accepted validation threshold of 2.0 Å for

successful redocking. This indicates that the docking protocol reliably reproduces the experimentally observed ligand binding orientation. Ligand redocking into the crystallographic binding

site was validated using RMSD calculations. The docked pose closely matches the experimental ligand orientation, confirming the reliability of the docking protocol employed [33]. A pharmacophore-level interpretation translates ligand docking results into an understanding of the key chemical features and spatial arrangements required for target binding, thereby helping to rationalize binding modes and guide future drug design [34].

Drug likeliness properties:

Drug likeliness is the analysis of the possibilities of the drug being delivered through the oral route of administration. Lipinski's rule of five indicates the drug's likelihood properties by assessing the drug's molecular descriptor values, all of which are limited to a factorial of five. Molecular weight of the drug should be <500 Daltons, partition coefficient <5, Hydrogen bond acceptors < 5, Hydrogen bond donors < 10 to deliver the drug through the oral route. More than 2 violations in the molecular descriptor make it impossible to deliver by the oral route [35]. Radar map of a drug molecule depicts the molecular size between 150 and 500 Daltons, Lipophilicity (-0.7 to +5), polarity

(20 to 130 A02), insolubility (-6 to 0), and insaturation (0.25 to 1 fraction of Csp3 bonds). Flexibility is indicated by the number of rotatable bonds (between 0 and 9). The colored zone is between the borders of the limits. If the physicochemical properties of the molecules cross the borderline, it will not be acceptable for the oral route of administration. Quercetin, apigenin, and luteolin violate the insaturation property due to a high number of unsaturations. Apigenin-7-glucoside and luteolin-7-glucoside violate the polarity property due to the addition of a glucose molecule at the 7th position [36].

Formulation Strategies and Alternative Delivery Methods for Lipinski's Rule-Violating Compounds:

Many bioactive flavonoids, particularly glycosylated derivatives like luteolin-7-O-glucoside and apigenin-7-O-glucoside, may violate one or more of Lipinski's "Rule of Five" due to high molecular weight, excess hydrogen bond donors/acceptors, or reduced lipophilicity, potentially limiting oral absorption. The following approaches improve the drug delivery and bioavailability of the flavonoids.

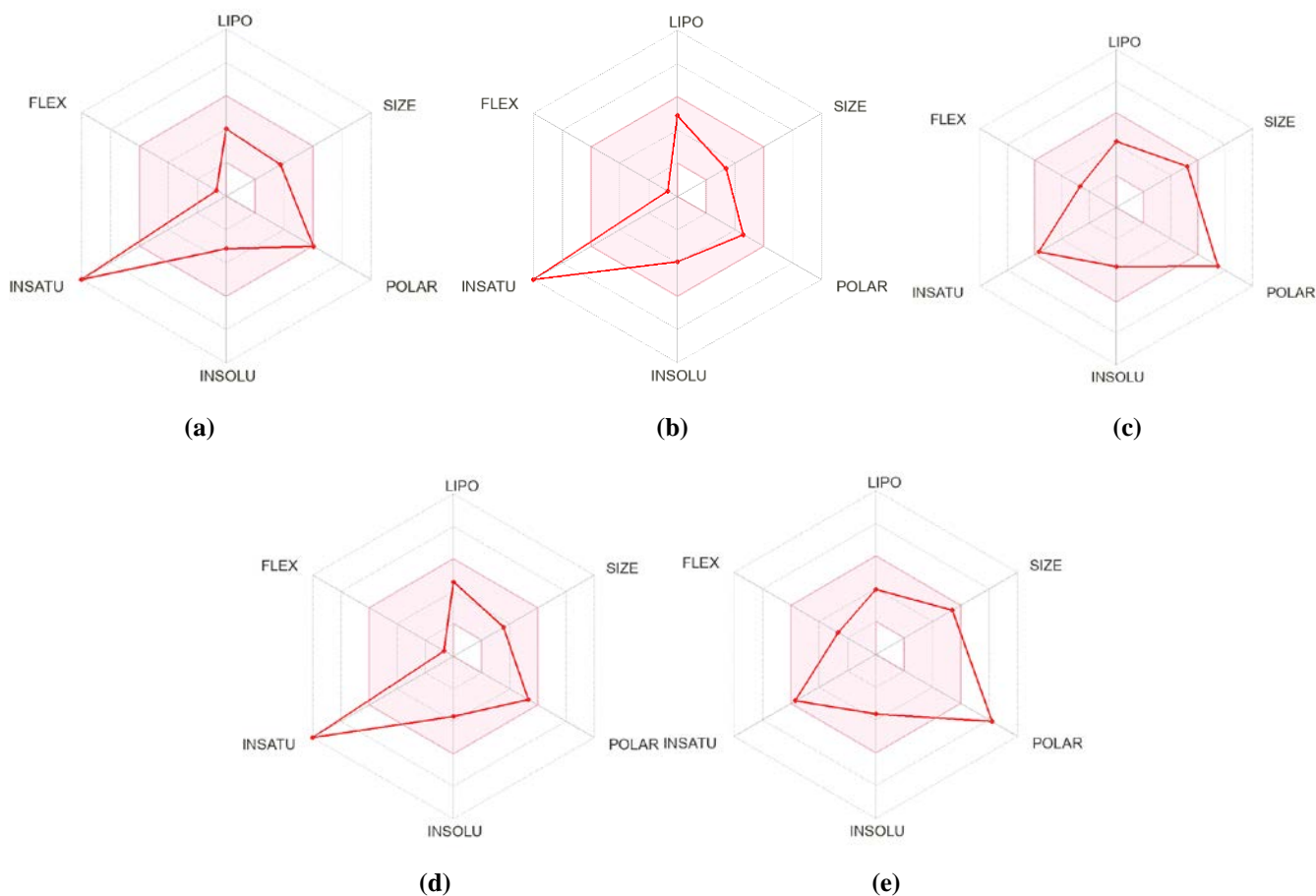


Figure 6: Drug likeliness radar maps of (a) Quercetin, (b) Apigenin, (c) Apigenin-7-glucoside, (d) Luteolin, and (e) Luteolin-7-glucoside.







 Nanocarrier Systems	<ul style="list-style-type: none"> Enhanced bioavailability Targeted delivery Reduced systemic toxicity
 Prodrug Design	<ul style="list-style-type: none"> Better oral uptake Controlled release Overcomes poor absorption and low permeability issues
 Transdermal/Topical Delivery	<ul style="list-style-type: none"> Bypasses GI degradation and first-pass metabolism Ideal for localized treatment of skin inflammation
 Cyclodextrin Complexation	<ul style="list-style-type: none"> Improved solubility, stability, and formulation performance Suitable for both oral and dermal deliver flavonoids
 Permeation Enhancers	<ul style="list-style-type: none"> Increased systemic exposure Improved oral bioavailability Supports systemic therapy by enhancing absorption
 Alternative Dosage Forms	<ul style="list-style-type: none"> Rapid onset Patient compliance Improves systemic availability of poorly permeable flavonoids

Figure 7: Strategies for flavonoid delivery in psoriasis, highlighting advanced formulation approaches such as nanocarriers, prodrugs, transdermal systems, cyclodextrin complexes, permeation enhancers, and alternative dosage forms to enhance bioavailability, stability, and targeted therapeutic efficacy.

CONCLUSION

Flavonoids, particularly quercetin, apigenin, luteolin-7-O-glucoside, and apigenin-7-O-glucoside, exhibit strong in silico binding affinities towards psoriasis-relevant targets, positioning them as promising lead candidates. Glycosides likely benefit from higher polarity and interaction potential, whereas aglycones may offer superior membrane permeability, suggesting complementary pharmacokinetic advantages and a feasible route for oral delivery.

ACKNOWLEDGEMENTS

The authors would like to express their sincere gratitude to Dr. Manikanta Murahari (KL University, Vaddeswaram, Guntur) and Dr. Ajitha Azhakesan (Sri Ramachandra School of Pharmacy, Porur, Chennai) for their continuous support, guidance, and valuable insights throughout this study.

FINANCIAL ASSISTANCE

NIL

CONFLICT OF INTEREST

The authors declare no conflict of interest.

AUTHOR CONTRIBUTION

All authors contributed significantly to the conception, collection of materials, development of methodology, analysis of results, and discussion. Venkata Rajesham Vallala contributed to the development of intellectual content and the buildup of ideology. Narendra Pentu participated in final draft proofreading and write-up improvement. Kishore Kumar was involved in the drafting of the article. Ashok Morsu is involved in the write-up process. Tadikonda Rama Rao is the principal advisor and moderator of literature screening.

REFERENCES

- [1] Guilloteau K, Paris I, Pedretti N, Boniface K, Juchaux F, Huguier V, Guillet G, Bernard F-X, Lecron J-C, Morel F. Skin Inflammation Induced by the Synergistic Action of IL-17A, IL-22, Oncostatin M, IL-1 α , and TNF- α Recapitulates Some Features of Psoriasis. *The Journal of Immunology*, **184**, 5263–70 (2010) <https://doi.org/10.4049/jimmunol.0902464>.
- [2] Griffiths CEM, Armstrong AW, Gudjonsson JE, Barker JNWN. Psoriasis. *The Lancet*, **397**, 1301–15 (2021) [https://doi.org/10.1016/S0140-6736\(20\)32549-6](https://doi.org/10.1016/S0140-6736(20)32549-6).
- [3] Iskandar IYK, Parisi R, Griffiths CEM, Ashcroft DM. Systematic review examining changes over time and variation in the incidence and prevalence of psoriasis by age and gender*. *British Journal of Dermatology*, **184**, 243–58 (2021) <https://doi.org/10.1111/bjd.19169>.
- [4] Capon F. The Genetic Basis of Psoriasis. *Int J Mol Sci*, **18**, 2526 (2017) <https://doi.org/10.3390/ijms18122526>.
- [5] Chen G, Lv C, Nie Q, Li X, Lv Y, Liao G, Liu S, Ge W, Chen J, Du Y. Essential Oil of *Matricaria chamomilla* Alleviate Psoriatic-Like Skin Inflammation by Inhibiting PI3K/Akt/mTOR and p38MAPK Signaling Pathway. *Clin Cosmet Investig Dermatol*, **17**, 59–77 (2024) <https://doi.org/10.2147/CCID.S445008>.
- [6] Rivera-Yañez CR, Ruiz-Hurtado PA, Mendoza-Ramos MI, Reyes-Realí J, García-Romo GS, Pozo-Molina G, Reséndiz-Albor AA, Nieto-Yañez O, Méndez-Cruz AR, Méndez-Catalá CF, Rivera-Yañez N. Flavonoids Present in Propolis in the Battle against Photoaging and Psoriasis. *Antioxidants*, **10**, 2014 (2021) <https://doi.org/10.3390/antiox10122014>.
- [7] Gębka N, Adamczyk J, Gębka-Kępińska B, Mizgała-Izworska E. The role of flavonoids in prevention and treatment of selected skin diseases. *Journal of Pre-Clinical and Clinical Research*, **16**, 99–107 (2022) <https://doi.org/10.26444/jpccr/152551>.
- [8] Chen G, Lv C, Nie Q, Li X, Lv Y, Liao G, Liu S, Ge W, Chen J, Du Y. Essential Oil of *Matricaria chamomilla* Alleviate Psoriatic-Like Skin Inflammation by Inhibiting PI3K/Akt/mTOR and

- p38MAPK Signaling Pathway. *Clin Cosmet Investig Dermatol*, **17**, 59–77 (2024) <https://doi.org/10.2147/CCID.S445008>.
- [9] Eberhardt J, Santos-Martins D, Tillack AF, Forli S. AutoDock Vina 1.2.0: New Docking Methods, Expanded Force Field, and Python Bindings. *J Chem Inf Model*, **61**, 3891–8 (2021) <https://doi.org/10.1021/acs.jcim.1c00203>.
- [10] Pingale RN, Pratyush K, Wagh B, Jain AA, Mailavaram RP. Evaluation of PPAR gamma agonists: A molecular docking and QSAR study of chalcone analog. *J Appl Pharm Sci*, **15**, 155-63 (2024) <https://doi.org/10.7324/JAPS.2024.190652>.
- [11] Trott O, Olson AJ. AutoDock Vina: Improving the speed and accuracy of docking with a new scoring function, efficient optimization, and multithreading. *J Comput Chem*, **31**, 455–61 (2010) <https://doi.org/10.1002/jcc.21334>.
- [12] Akachukwu I, Amara EE. In-silico study of flavonoids from Cassia tora as potential anti-psoriatic agent. *J Appl Pharm Sci*, **9**, 82–7 (2019) <https://doi.org/10.7324/JAPS.2019.90410>.
- [13] Lipinski CA. Lead- and drug-like compounds: the rule-of-five revolution. *Drug Discov Today Technol*, **1**, 337–41 (2004) <https://doi.org/10.1016/j.ddtec.2004.11.007>.
- [14] Shaikh GM, Murahari M, Thakur S, Kumar MS, YC M. Studies on ligand-based pharmacophore modeling approach in identifying potent future EGFR inhibitors. *J Mol Graph Model*, **112**, 108114 (2022) <https://doi.org/10.1016/j.jmgm.2021.108114>.
- [15] Karoui S, Khaoua O, Benbellat N, Antonczak S, Messaoudi A. Molecular Docking, Molecular Dynamics, pkCSM Drug-Likeness Profiles, Toxicity, and DFT Study of the Antioxidant and Anticancer Activities of Three Flavonoid Derivatives. *ChemistrySelect*, **9**, (2024) <https://doi.org/10.1002/slct.202401776>.
- [16] Muhammed MT, Aki-Yalcin E. Molecular Docking: Principles, Advances, and Its Applications in Drug Discovery. *Lett Drug Des Discov*, **21**, 480–95 (2024) <https://doi.org/10.2174/1570180819666220922103109>.
- [17] Pentu N, Rishitha P, Nikhil G, Rao TR. Therapeutic potential of flavonoids in the management of psoriasis. *Asian J Pharm Pharmacol*, **10**, 35–45 (2024) <https://doi.org/10.31024/ajpp.2024.10.1.2>.
- [18] Tyagi V, Singh VK, Sharma PK, Singh V. Essential oil-based nanostructures for inflammation and rheumatoid arthritis. *J Drug Deliv Sci Technol*, **60**, (2020) <https://doi.org/10.1016/j.jddst.2020.101983>.
- [19] Monteiro Espíndola KM, Ferreira RG, Mosquera Narvaez LE, Rocha Silva Rosario AC, Machado Da Silva AH, Bispo Silva AG, Oliveira Vieira AP, Chagas Monteiro M. Chemical and pharmacological aspects of caffeic acid and its activity in hepatocarcinoma, Frontiers Media S.A., 9, 541., (2019). <https://doi.org/10.3389/fonc.2019.00541>
- [20] Niazi A, Baradaran Rahimi V, Askari N, Rahmanian-Devin P, Askari VR. Topical treatment for the prevention and relief of nipple fissure and pain in breastfeeding women: A systematic review. *Adv Integr Med*, **8**, 312–21 (2021) <https://doi.org/10.1016/j.aimed.2021.07.001>.
- [21] Chandran SS, Kealey JT, Reeves CD. Microbial production of isoprenoids. *Process Biochemistry*, **46**, 1703–10 (2011) <https://doi.org/10.1016/j.procbio.2011.05.012>.
- [22] Jasemi SV, Khazaei H, Morovati MR, Joshi T, Aneva IY, Farzaei MH, Echeverría J. Phytochemicals as treatment for allergic asthma: Therapeutic effects and mechanisms of action. *Phytomedicine*, **122**, 155149 (2024) <https://doi.org/10.1016/j.phymed.2023.155149>.
- [23] Rehmat S, Khera RA, Hanif MA, Ayub MA, Zubair M. Chamomilla. *Medicinal Plants of South Asia: Novel Sources for Drug Discovery*, 101–12 (2019) <https://doi.org/10.1016/B978-0-08-102659-5.00008-2>.
- [24] Akachukwu I, Amara EE. In-silico study of flavonoids from Cassia tora as potential anti-psoriatic agent. *J Appl Pharm Sci*, **9**, 82–7 (2019) <https://doi.org/10.7324/JAPS.2019.90410>.
- [25] Zafar F, Gupta A, Thangavel K, Khatana K, Sani AA, Ghosal A, Tandon P, Nishat N. Physicochemical and Pharmacokinetic Analysis of Anacardic Acid Derivatives. *ACS Omega*, **5**, 6021–30 (2020) <https://doi.org/10.1021/acsomega.9b04398>.
- [26] Kenny PW. Hydrogen-Bond Donors in Drug Design. *J Med Chem*, **65**, 14261–75 (2022) <https://doi.org/10.1021/acs.jmedchem.2c01147>.
- [27] Coimbra JTS, Feghali R, Ribeiro RP, Ramos MJ, Fernandes PA. The importance of intramolecular hydrogen bonds on the translocation of the small drug piracetam through a lipid bilayer. *RSC Adv*, **11**, 899–908 (2020) <https://doi.org/10.1039/d0ra09995c>.
- [28] Azzam K AL. SwissADME and pkCSM Webservers Predictors: an integrated Online Platform for Accurate and Comprehensive Predictions for In Silico ADME/T Properties of Artemisinin and its Derivatives. *Kompleksnoe Ispol'zovanie Mineral'nogo syr'â/Complex Use of Mineral Resources/Mineraldik Shikisattardy Keshendi Paidalanu*, **325**, 14–21 (2023) <https://doi.org/10.31643/2023/6445.13>.
- [29] Karoui S, Khaoua O, Benbellat N, Antonczak S, Messaoudi A. Molecular Docking, Molecular Dynamics, pkCSM Drug-Likeness Profiles, Toxicity, and DFT Study of the Antioxidant and Anticancer Activities of Three Flavonoid Derivatives. *ChemistrySelect*, **9**, (2024) <https://doi.org/10.1002/slct.202401776>.
- [30] Pires DEV, Blundell TL, Ascher DB. pkCSM: Predicting small-molecule pharmacokinetic and toxicity properties using graph-based signatures. *J Med Chem*, **58**, 4066–72 (2015) <https://doi.org/10.1021/acs.jmedchem.5b00104>.
- [31] Hevener KE, Zhao W, Ball DM, Babaoglu K, Qi J, White SW, Lee RE. Validation of molecular docking programs for virtual

- screening against dihydropteroate synthase. *J Chem Inf Model*, **49**, 444-60 (2009) <https://doi.org/10.1021/ci800293n>
- [32] Eberhardt J, Santos-Martins D, Tillack AF, Forli S. AutoDock Vina 1.2.0: New Docking Methods, Expanded Force Field, and Python Bindings. *J Chem Inf Model*, **61**, 3891–8 (2021) <https://doi.org/10.1021/acs.jcim.1c00203>.
- [33] Yang S-Y. Pharmacophore modeling and applications in drug discovery: challenges and recent advances. *Drug Discov Today*, **15**, 444–50 (2010) <https://doi.org/10.1016/j.drudis.2010.03.013>.
- [34] Lipinski CA. Drug-like properties and the causes of poor solubility and poor permeability. *J Pharmacol Toxicol Methods*, **44**, 235–49 (2000) [https://doi.org/10.1016/S1056-8719\(00\)00107-6](https://doi.org/10.1016/S1056-8719(00)00107-6).
- [35] Daina A, Michielin O, Zoete V. SwissADME: a free web tool to evaluate pharmacokinetics, drug-likeness and medicinal chemistry friendliness of small molecules. *Sci Rep*, **7**, 42717 (2017) <https://doi.org/10.1038/srep42717>.

Supplementary Data:

Table 1: List of ligands with their SMILES notations.

Name of the compound	Pubchem ID	SMILES
Quercetin	5280343	<chem>C1=CC(=C(C=C1C2=C(C(=O)C3=C(C=C(C=C3O2)O)O)O)O)O</chem>
apigenin	5280443	<chem>C1=CC(=CC=C1C2=CC(=O)C3=C(C=C(C=C3O2)O)O)O</chem>
Apigenin 7-glucoside	578-74-5	<chem>C1=CC(=CC=C1C2=CC(=O)C3=C(C=C(C=C3O2)O[C@@H]4[C@@H]([C@@H]([C@@H]([C@@H](O4)CO)O)O)O)O)O</chem>
Luteolin	5280445	<chem>C1=CC(=C(C=C1C2=CC(=O)C3=C(C=C(C=C3O2)O)O)O)O</chem>
Luteolin-7-O-glucoside	5280637	<chem>C1=CC(=C(C=C1C2=CC(=O)C3=C(C=C(C=C3O2)O[C@@H]4[C@@H]([C@@H]([C@@H]([C@@H](O4)CO)O)O)O)O)O)O</chem>
Matricin	92265	<chem>C[C@H]1[C@@H]2[C@H](CC(=C3C=C[C@@]([C@@H]3[C@H]2OC1=O)(C)O)C)OC(=O)C</chem>
Chamazulene	10719	<chem>CCC1=CC2=C(C=CC2=C(C=C1)C)C</chem>
Caffeic acid	689043	<chem>C1=CC(=C(C=C1/C=C/C(=O)O)O)O</chem>
Guaiazulene	3515	<chem>CC1=C2C=CC(=C2C=C(C=C1)C(C)C</chem>
Isobutyl angelate	5367807	<chem>C/C=C(/C)\C(=O)OCC(C)C</chem>
Farnesene	5281516	<chem>CC(=CCC/C(=C/C/C=C(/C)/C=C)/C)C</chem>
Beta-farnesene	5281517	<chem>CC(=CCC/C(=C/CCC(=C)C=C)/C)C</chem>
Farnesol	445070	<chem>CC(=CCC/C(=C/CC/C(=C/CO)/C)/C)C</chem>
alpha-Bisabolol	1549992	<chem>CC1=CC[C@@H](CC1)[C@@](C)(CCC=C(C)C)O</chem>
Umbelliferone	5281426	<chem>C1=CC(=CC2=C1C=CC(=O)O2)O</chem>
Herniarin	10748	<chem>COC1=CC2=C(C=C1)C=CC(=O)O2</chem>

Table 2: Protein code with GRID coordinates.

Protein PDB code	Protein	GRID coordinates
2AZ5	TNF- α	-19.410, 74.651, 33.850
3QWR	IL-23	24.346980, -28.225320 -51.874320
5HI4	IL-17A	80.731080, -43.501432 -45.735545
5K1I	PDE-4	12.576071, 3.744179

		67.719607
4OTF	BTK	-38.572442, 27.147767 -10.124349
5TTS	JAK-3	-0.164050, 16.815400 -4.872050
5FUC	IL-6	-13.200714, 1.798643 44.180286
2C6O	P38MAPK	11.247857, -9.390714 9.959036